Journal of Structural Geology 115 (2018) 304–310

Contents lists available at ScienceDirect

Journal of Structural Geology

journal homepage: www.elsevier.com/locate/jsg

Interference fold patterns in regional unidirectional stress fields: A result of local kinematic interactions

Sergio P. Neves*, Tiago A.S. Santos, Paulo C. Medeiros, Laís Q. Amorim, Dionísio C.G. Casimiro

Departamento de Geologia, Universidade Federal de Pernambuco, 50740-530, Recife, Brazil

ARTICLE INFO

Keywords:
Kinematic analysis
Shear zones
Superposed folds

ABSTRACT

Folds are commonly found in association with ductile shear zones. However, superimposed folding contemporaneous with shearing is rarely reported. Here, we describe a macroscopic fold interference pattern with geometry intermediate between types 1 and 2 related to development of adjacent transcurrent shear zones. The interference fold pattern is located in a compartment bounded, on the eastern side, by an ENE-trending, dextral shear zone that connects with a NE-trending, sinistral shear zone, and, on the western side, by a NE-trending sinistral shear zone. A first folding episode produced NW-trending, SW-verging inclined folds and a later one NE-trending, upright folds. Folds of the first event are attributed to a local contractional strain field induced by the growth of the shear zones with opposed kinematics whereas the later folding episode and nucleation of the western shear zone reflects regional NW-SE contraction. Folding of a macro-scale NW-trending fold by NE-trending folds produced the fold interference structure. In contrast with most cases of types 1 and 2 fold interference patterns, in the present case no change on the orientation of regional stress axes is required.

1. Introduction

Since the seminal work of Ramsay (1967), interference patterns resulting from refolding of preexisting folds by a new folding event have been recognized in a number of cases worldwide (e.g., Forbes et al., 1984; Simón, 2004 and references therein). Refold structures are commonly divided into types 1, 2 and 3 according to the relative orientations of the two folding phases, which produce interference patterns in horizontal surfaces referred to as "dome-and-basin", "crescent" and "coaxial" or "hook", respectively (Ramsay, 1967; Thiessen, 1986). Refolding may be a consequence of progressive deformation at constant orientation of the main stress axes, producing type 3 fold interference patterns (e.g., Baird and Shrady, 2011). In the cases of types 1 and 2 fold interference patterns, however, polyphase deformation is usually invoked, and results from different orientations of the main stress axes (Ramsay and Huber, 1987). This variation may occur by rotation of the stress axes during a single orogenic event (e.g., Kolb et al., 2013) or may reflect different boundary conditions resulting from separate orogenies (e.g., Lahtinen et al., 2015).

Another structural feature largely documented since the 1970's is the association of folds with ductile shear zones (e.g., Escher and Watterson, 1974; Kärki and Laajoki, 1995; Graseman and Stüwe, 2001; Carreras et al., 2005; Van Kranendonk et al., 2013). However, superposed folding contemporaneous with shearing is rarely reported (e.g., Zhang and Cunningham, 2012; Van Kranendonk et al., 2013). The Neoproterozoic Borborema Province (northeastern Brazil) is an ideal place to study the connection between folding and strike-slip shearing since it contains a complex network of ductile transcurrent shear zones (Vauchez et al., 1995). For instance, Corsini et al. (1996) described en-echelon, asymmetric folds developed in unmylonitized lenses wrapped around by sigmoidal shear zones whereas Neves et al. (2005) and Archanjo et al. (2008) interpreted macroscopic NE-trending, upright folds between shear zones as being contemporaneous with strike slip-shearing.

One case of refolded folds in the Borborema Province was described by Neves et al. (2017). They attributed formation of NW-trending folds to contraction at the leading edge of a propagating NE-trending sinistral shear zone. The folds were subsequently refolded by NE-trending folds during progressive deformation resulting from bulk NW-SE shortening. Here we expand the area studied in this previous paper and describe a macroscopic fold interference pattern with geometry intermediate between types 1 and 2, referred from now on as the Caroalina fold in-

* Corresponding author.
E-mail addresses: serpane@hotlink.com.br, sergio@pq.cnpq.br (S.P. Neves).

https://doi.org/10.1016/j.jsg.2018.04.012
Received 22 December 2017; Received in revised form 23 March 2018; Accepted 6 April 2018
Available online 26 April 2018

terference structure. It will be demonstrated that development of the fold interference pattern does not necessarily require variation in the orientation of the regional stress axes, being kinematically controlled by nearby local transcurrent shear zones.

2. Geological setting

The study area is located in the Central Subprovince of the Borborema Province, a region well-known for presence of conjugate dextral and sinistral shear zones with lengths of tens to hundreds of kilometers (Vauchez et al., 1995; Neves and Mariano, 1999; Silva and Mariano, 2000; Neves et al., 2005; Archanjo et al., 2008). The Central Subprovince is divided into four tectonic domains (Fig. 1a). The Caroalina fold interference structure is located in the Alto Moxotó Domain, which is separated from the Rio Capibaribe Domain in the east by the Congo-Cruzeiro do Nordeste shear zone system (Fig. 1b). The Alto Moxotó Domain consists mainly of high-grade, commonly migmatized, orthogneisses and metasedimentary rocks (Santos et al., 2002, 2015, 2004; Neves et al., 2015, 2017). Orthogneisses, thought to represent the basement upon which the supracrustal rocks were deposited, have dominant ages ranging from 2.15 to 2.00 Ga (Santos et al., 2004, 2015; Neves et al., 2015, 2017), with local occurrence of Early Proterozoic and Archean rocks (Santos et al., 2015, 2017a). Metasedimentary rocks consist mainly of biotite schist and paragneiss, with subordinate quartzite, marble and calc-silicate rocks. Regional deformation and metamorphism related to the Brasiliano Orogeny is loosely constrained to the interval 642-590 Ma by the ages of, respectively, the youngest detrital zircons and metamorphic zircons in metasedimentary sequences (Neves et al., 2017).

Two generations of outcrop-scale, pre-strike slip shearing fabrics are recognized in the Alto Moxotó Domain (Neves et al., 2017; this work). An early deformation phase is only documented by the presence of intrafolial, tight to isoclinal folds that deform a previous metamorphic foliation. The dominant foliation (S_2) is thus attributed to a second phase of deformation (D_2). This foliation is shared by orthogneisses and metasedimentary rocks and locally intensifies into centimeter-to decameter-wide belts of mylonites (Fig. 2a). In places where S_2 is preserved from subsequent folding events, it has shallow to moderate dip (Fig. 1b) and the associated stretching lineation trends W to WNW, with shear sense criteria indicating westward tectonic transport direction (Fig. 2a and b). A third phase of deformation is represented by folding of S_2 by overturned to recumbent, open to tight folds (Fig. 2c) that locally show type 3 fold interference patterns with F_2 folds (Fig. 6a of Neves et al., 2017).

3. Shear zones, map-scale fold interference pattern and mesoscopic fabrics

3.1. Shear zones

The Caroalina fold interference structure is located between the Congo-Cruzeiro do Nordeste shear zone system and the NE-trending

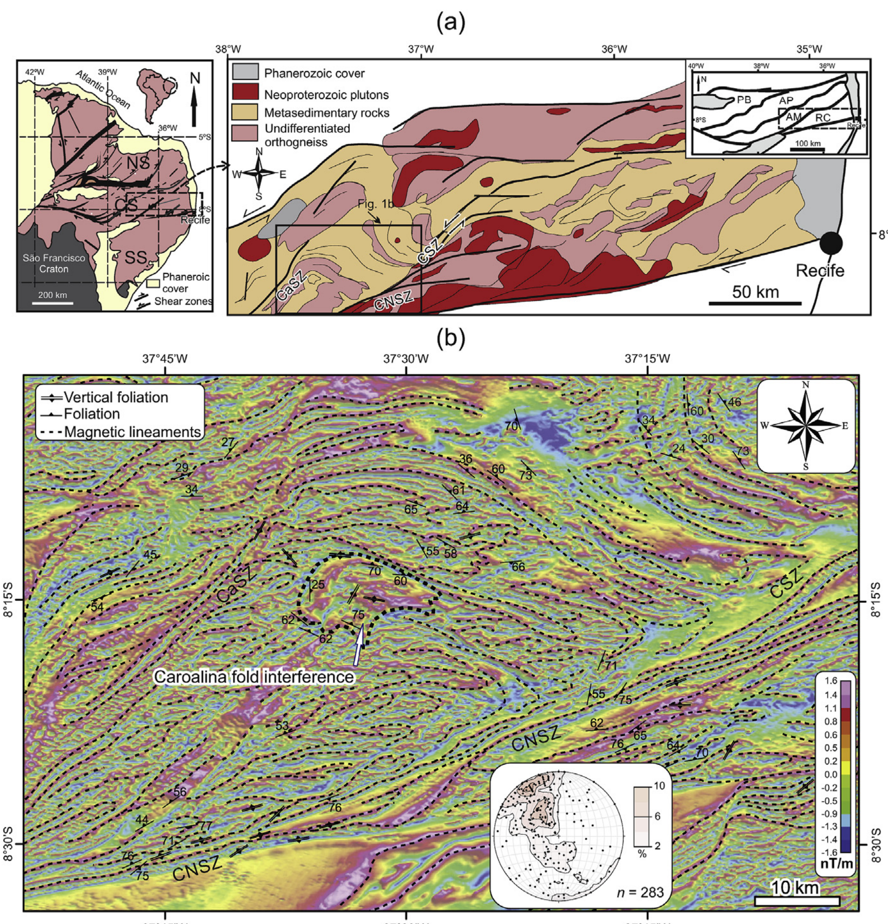

Fig. 1. (a) Sketches showing the subdivision of the Borborema Province in Northern (NS), Central (CS) and Southern (SS) subprovinces and simplified geological map of the Alto Moxotó and Rio Capibaribe domains. Shear zones referred in the text: CSZ, Congo; CNSZ, Cruzeiro do Nordeste; CaSZ, Caiçara. Inset shows the subdivision of the Central Subprovince in the Piancó-Alto Brígida (PB), Alto Pajeú (AP), Alto Moxotó (AM) and Rio Capibaribe (RC) domains. (b) Colour image of the tilt derivative of aeromagnetic data (see Santos et al., 2017b, for data acquisition, processing and terminology), with superposed magnetic lineaments and foliations. Inset shows poles to foliations in equal area, lower hemisphere stereographic projection. (For interpretation of the references to colour in this figure legend, the reader is referred to the Web version of this article.)

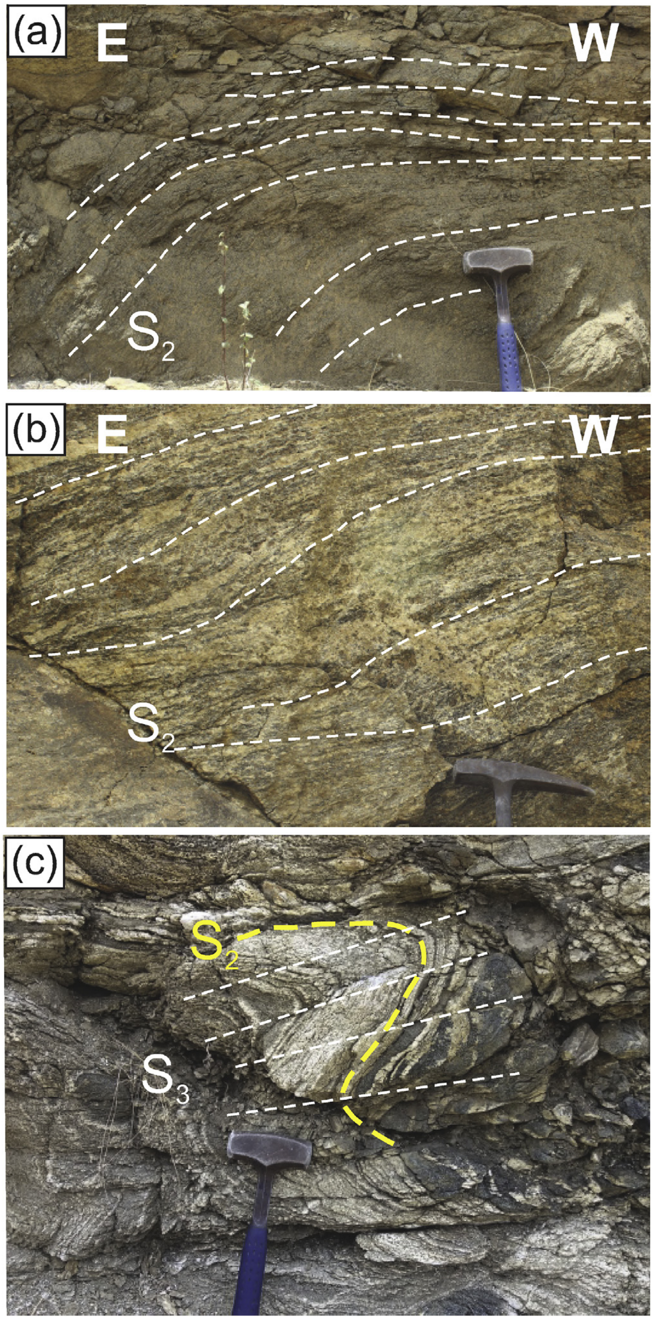

Fig. 2. Field aspects of pre-shear zone-related structures in the study area. (a, b) Sigmoidal S_2 foliation indicating top-to-the-W tectonic transport. In (a), the foliation intensifies into a mylonitic fabric (top of photo). (c) Folding of S_2 by close, recumbent fold displaying a weak axial-plane foliation (S_3).

Caiçara shear zone (Fig. 1b). Previous works consider the Congo and Cruzeiro do Nordeste shear zones as a single, sinistral shear zone, inflecting southwestward from a NE trend to an ENE one (Santos et al., 2002; Santos and Accioly, 2010; Santos, 2012). Alike other shear zones with similar orientation in the Central Subprovince, the sinistral kinematics of the Congo shear zone (CSZ) is well-established (Santos et al., 2002; Santos and Accioly, 2010; Santos, 2012). However, based on interpretation of aeromagnetic data and field and microstructural work, here we demonstrate that the Cruzeiro do Nordeste shear zone (CNSZ) is dextral, such that these shear zones constitute a conjugate pair with opposite kinematics.

Fig. 3a shows clearly the curvature of magnetic lineaments at the western terminus of the CNSZ, defining folds with a south-facing concavity, consistent with dextral shear. This is in contrast to the anticlockwise rotation of magnetic lineaments in the Northeast due to the sinistral drag of the CSZ (Fig. 1b). The boundaries of the CNSZ, defined by the first appearance of a mylonitic fabric observed in the field (Fig. 3c), together with the trend of magnetic lineaments inside it, define a large S-C structure, also indicating dextral shear. Protoliths of mylonites include orthogneiss, coarse-grained to pegmatitic granite and fine-to medium-grained equigranular granite. Kinematic indicators at mesoscopic and microscopic scales corroborate the macroscopic-scale shear criteria (Fig. 3). S-C and S-C-C′ fabrics (Fig. 3c, i-iv), syn-mylonitic asymmetric Z-type folds (Fig. 3c, v), asymmetric boudins, and sigmoids (Fig. 3, iv) are common at the mesoscale, with shear sense becoming less clear only in ultramylonites. At the microscopic scale, oblique foliation in quartz ribbons (Fig. 3, vi) and σ-type porphyroclasts (Fig. 3c, vii) are ubiquitous, and δ-type porphyroclasts (Fig. 3c, vi) are occasionally observed.

The Caiçara shear zone (CaSZ) terminates northeastward inside the study area (Fig. 1a). Rotation of the regional foliation and magnetic lineaments (Fig. 1b), as well as mesoscopic shear sense indicators, clearly show its sinistral character.

3.2. The Caroalina fold interference structure

The Caroalina fold interference structure is delineated by micaschist and quartzite of the Caroalina Complex surrounded by Paleoproterozoic orthogneisses of the Floresta and Cabaceiras complexes (Fig. 4). In the core and rim of the structure, S_2 has dominant moderate to steep dips to the N, with steeper dips in the northern side indicating that the main architecture is that of a large, south-verging synform (Fig. 4). NE-SW-striking folds affected the orientation of this early formed fold, causing the curvature of its axial trace and forming an intermediate 1–2 fold interference pattern. Poles to S_2 plotted on a stereographic diagram generate a great circle with a pole 030°, 70° (azimuth, plunge), representing the axis of the younger folding event (Fig. 4). Together with the fold axial trace of c. 035°, this axis allow to calculate an axial plane 330°, 85° (dip direction, dip).

Two sets of inclined to upright folds are also observed at outcrop scale. E-W to NW-SE-striking folds have axial planes steeply dipping northwards with hinge lines showing shallow to steep plunges (Figs. 4 and 5a, b), probably as a result of modification associated with the younger folding event. They range from open to tight, with development of a strong axial plane foliation in sites of higher strain (Fig. 5a). NE-SW-striking folds generally are more open and have hinge lines with steep plunges (Figs. 4 and 5c), characteristic of shear zone-related folds. Type 2 fold interference patterns are locally observed (Fig. 5d).

4. Discussion

Structures and fabrics in the Alto Moxotó Domain have mostly NW-SE direction, contrasting with the dominant NE trend throughout the Central Subprovince (Fig. 1b). Development of NW-trending folds in an area to the northeast of the present one was interpreted by Neves et al. (2017) as forming at the front of the southwestward propagating CSZ. It is now considered more probable that these folds were produced due to

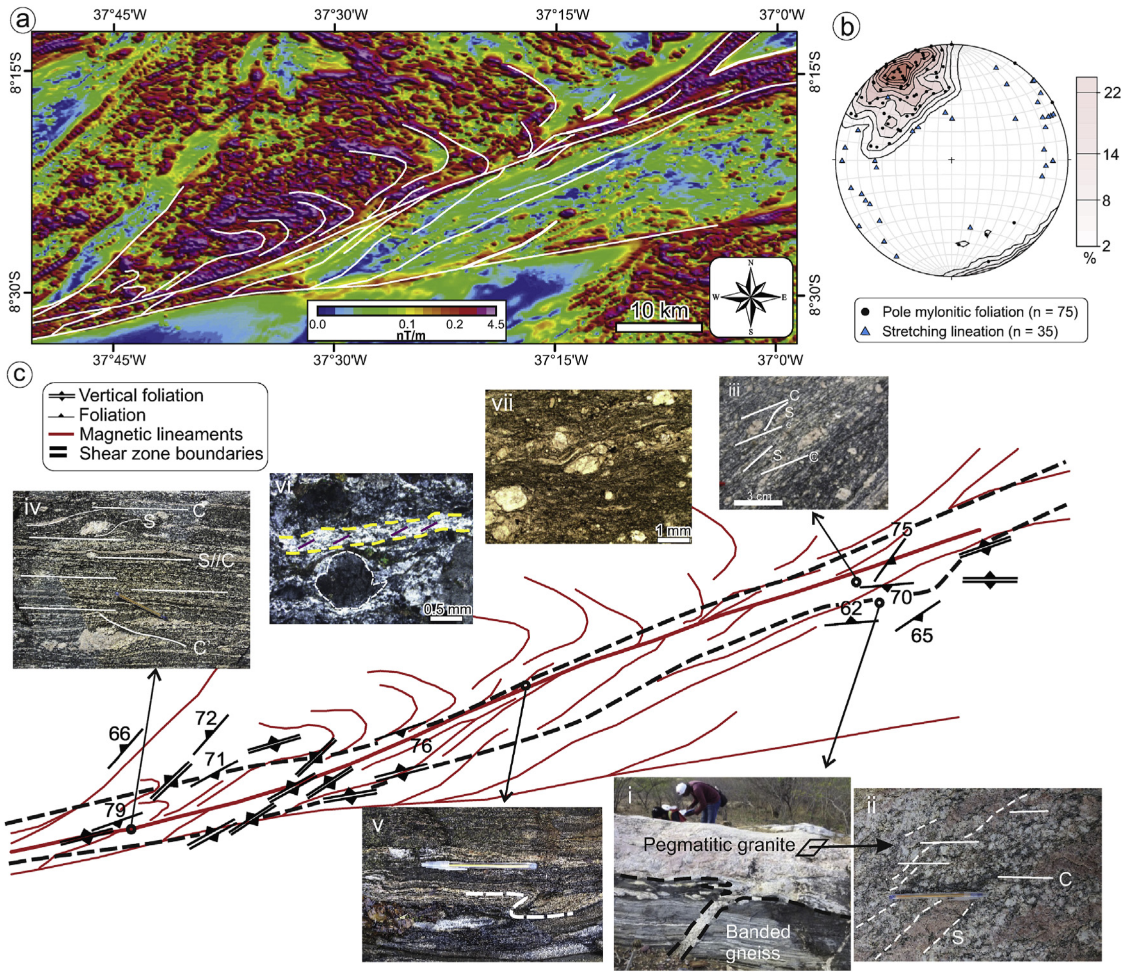

Fig. 3. (a) Colour image of the analytic signal amplitude of the total magnetic field with superposed magnetic lineaments (see Santos et al., 2017b, for data acquisition, processing and terminology). (b) Lower hemisphere, equal area projection of poles to mylonitic foliation (n = 75) and stretching lineations (n = 35) along the Cruzeiro do Nordeste shear zone (CNSZ). (c) Representative photographs of shear sense criteria indicating dextral shear in the CNSZ. Boundaries of the CNSZ as determined from the first appearance of mylonitic foliation in the field. (i, ii) Banded orthogneiss with sub-horizontal foliation capped by protomylonitic pegmatitic granite, which shows (ii) S-C fabric. (iii) Granitic S-C mylonite. (iv) Mylonitic gneiss with S-C fabric (top of photo), C′-type shear band (parallel to pencil) and sigmoid of quartz-feldspar aggregate (base of photo). (v) Asymmetric Z fold. (vi) Quartz ribbon with oblique foliation and δ-type porphyroclast (photomicrograph in crossed polarized light). (vii) σ-type porphyroclasts (photomicrograph in plain polarized light). (For interpretation of the references to colour in this figure legend, the reader is referred to the Web version of this article.)

a local contractional strain field resulting from nucleation and growth of shear zones with opposed kinematics (Fig. 6a). In fact, the dextral and sinistral kinematics of, respectively, CNSZ and CSZ require a dominant pure shear regime in the block located at their left side. The resulting NE-SW contraction can explain the anomalous orientation of structures in this portion of the Central Subprovince. The lack of offset of one shear zone by the other indicates that movement in the CNSZ and CSZ has not continued after their intersection. Since relative displacements are not observed, this suggests that deformation was relocated elsewhere after they merged. . We propose that nucleation of the Caiçara shear zone occurred at a late stage, associated with development of NE-trending folds, ultimately leading to formation of the Caroalina fold interference structure (Fig. 6b).

Field observations integrated with regional structural analysis (Ramsay and Huber, 1987; Mukhopadhyay and Haimanot, 1989) as well as theoretical considerations (Zheng et al., 2004, 2011) show that, in the ductile field, the maximum compressive stress bisects the obtuse angle between conjugate shear zones, although it is possible that the original angle was about 90° and increased during progressive deformation (Carreras et al., 2010). Therefore, the orientation of the CNSZ and CSZ suggests that the maximum compressive stress was approximately NW-SE and the formation of the Caroalina interference structure does not require any modification in the orientation of the regional stress axes between the first and second folding events.

5. Conclusion

Field work in combination with analysis of aeromagnetic data show that the Congo (CSZ) and Cruzeiro do Nordeste (CNSZ) shear zones constitute a conjugate pair of transcurrent shear zones with sinistral

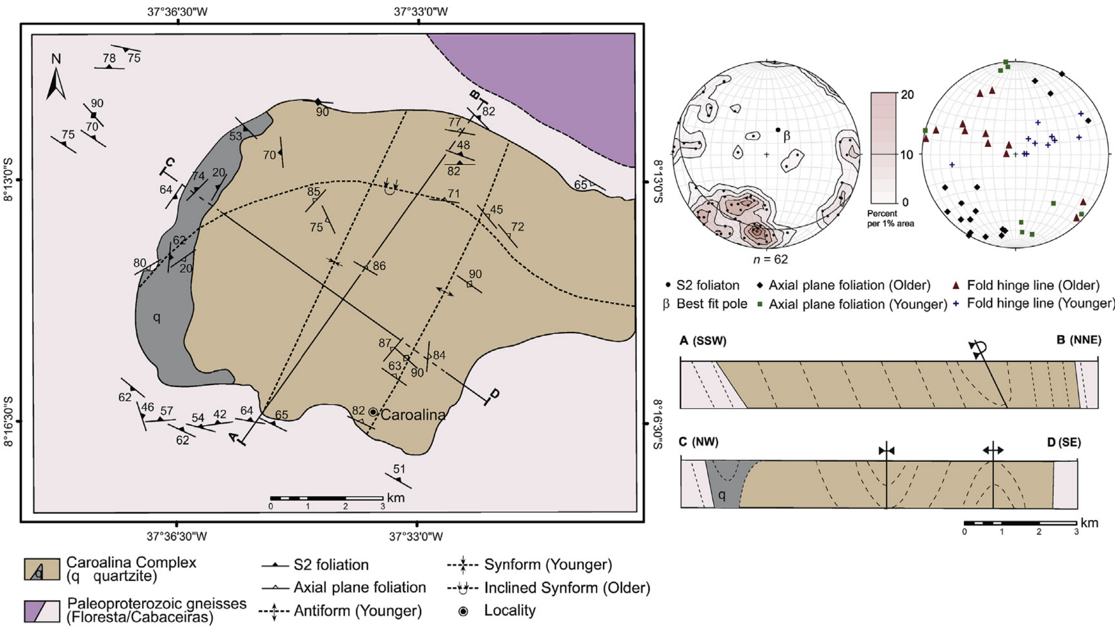

Fig. 4. Geological map of the Caroalina fold interference structure. Lower hemisphere stereographic plots show poles to foliations, with calculated β axis, and fold orientation data.

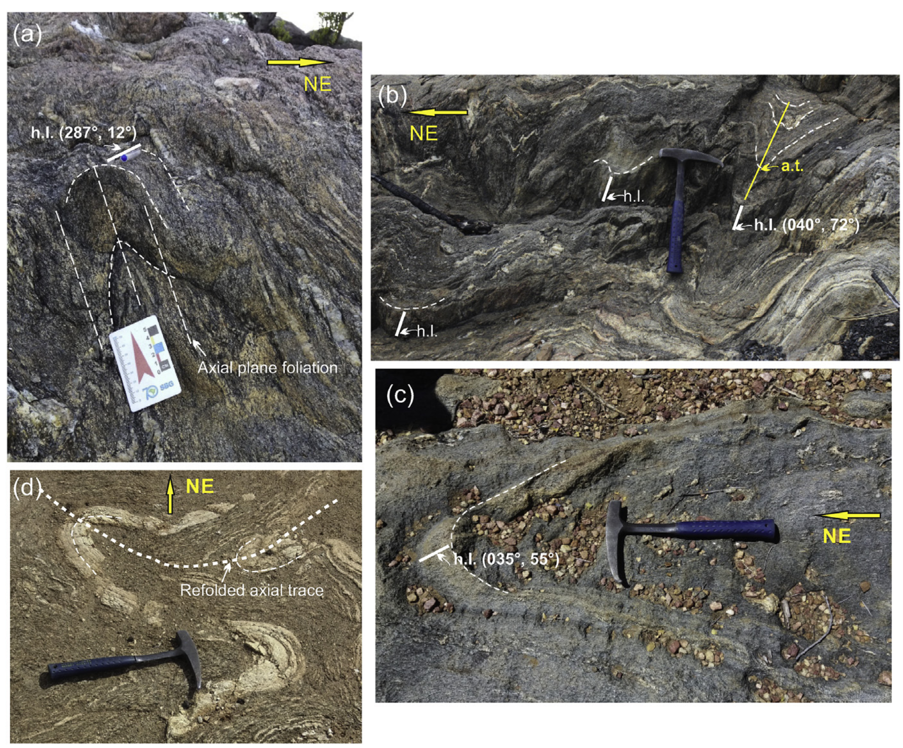

Fig. 5. Field aspects of shear zone-related folds. (a, b) SW-verging inclined folds with shallow (a) and steep (b) hinge lines. Note strong axial plane foliation in (a). h.l., hinge line; a.t., axial trace. (c) Upright NE-trending fold. (d) Tight fold refolded by NE-trending open fold.

and dextral kinematics, respectively. Lack of relative displacements at their junction attests their contemporaneous development, which induced a local contractional strain field at their left side and formation of NW-trending, SW-verging inclined folds. One macro-scale fold was subsequently refolded by upright, NE-trending folds coeval with a new sinistral shear zone, resulting in a macroscopic fold interference pattern. Formation of the Caroalina fold interference structure was thus controlled by nearby shear zones, requiring no rotation of the regional stress axes, with the maximum compressive stress remaining in an approximate NW-SE direction throughout the time of its development.

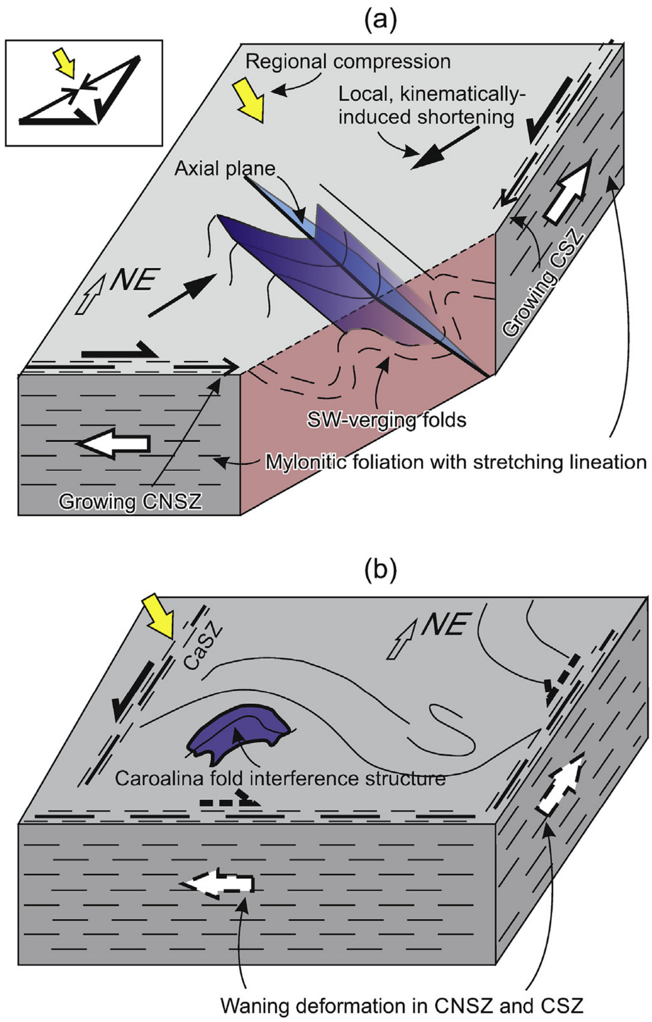

Fig. 6. Schematic block diagrams showing the proposed sequential development of structures in the study area. Inset in (a) shows the shortening direction resulting from the opposed kinematics of the Congo (CSZ) and Cruzeiro do Nordeste (CNSZ) shear zones. The actual angle between the shear zones is greater than shown in the block diagrams, where it was diminished to facilitate visualization. (a) Interference between the growing CSZ and CNSZ induces a local contractional strain field at their northwestern side, promoting development of SW-verging inclined folds. Depicted folds are not meant to represent real structures, only to illustrate the style of meso- and macroscale SW-verging folds. (b) After they intersect, movement is blocked in the CSZ and CNSZ; NW-SE regional compression leads to nucleation of the Caiçara shear zone (CaSZ), refolding of NW-trending folds by NE-trending folds, and development of the Caroalina fold interference structure. Between (a) and (b) the direction of regional compression remains unchanged (yellow arrow). (For interpretation of the references to colour in this figure legend, the reader is referred to the Web version of this article.)

Acknowledgements

SPN thanks João Hippertt for the invitation to submit an article to this special issue of Journal of Structural Geology. We also thank CPRM – *Serviço Geológico do Brasil* – for providing access to geophysical data for academic purposes, and constructive comments by two anonymous reviewers. This work was funded by research grant 449447/2014-6 from the Brazilian agency *Conselho Nacional de Desenvolvimento Científico e Tecnológico* (CNPq). TASS, LQA and PCM acknowledge scholarship from CNPq, and DCGC from *Fundação de Amparo ao Desenvolvimento Científico e Tecnológico do Estado de Pernambuco* (FACEPE).

References

Archanjo, C.J., Hollanda, M.H.B.M., Rodrigues, S.W.O., Brito Neves, B.B., Armstrong, R., 2008. Fabrics of pre- and syntectonic granite plutons and chronology of shear zones in the Eastern Borborema Province, NE Brazil. J. Struct. Geol. 30, 310–326.
Baird, G.B., Shrady, C.H., 2011. Timing and kinematics of deformation in the northwest adirondack lowlands, New York state: implications for terrane relationships in the southern Grenville Province. Geosphere 7, 1303–1323.
Carreras, J., Druguet, E., Griera, A., 2005. Shear zone-related folds. J. Struct. Geol. 27, 1229–1251.
Carreras, J., Czeck, D.M., Druget, E., Hudleston, P.J., 2010. Structure and development of an anastomosing network of ductile shear zones. J. Struct. Geol. 32, 656–666.
Corsini, M., Vauchez, A., Caby, R., 1996. Ductile duplexing at a bend of a continental-scale strike-slip shear zone: example from NE Brazil. J. Struct. Geol. 18, 385–394.
Escher, A., Watterson, J., 1974. Stretching fabrics, folds and crustal shortening. Tectonophysics 22, 223–231.
Forbes, C.J., Betts, P.G., Lister, G.S., 1984. Synchronous development of Type 2 and Type 3 fold interference patterns: evidence for recumbent sheath folds in the Allendale Area, Broken Hill, NSW, Australia. J. Struct. Geol. 26, 113–126.
Graseman, B., Stüwe, K., 2001. The development of flanking folds during simple shear and their use as kinematic indicators. J. Struct. Geol. 23, 715–724.
Kärki, A., Laajoki, K., 1995. An interlinked system of folds and ductile shear zones – late stage Svecokarelian deformation in the central Fennoscandian Shield, Finland. J. Struct. Geol. 17, 1233–1247.
Kolb, J., Thrane, Bagas, L., 2013. Field relationship of high-grade Neo- to Mesoarchaean rocks of South-East Greenland: tectonometamorphic and magmatic evolution. Gondwana Res. 23, 471–492.
Lahtinen, R., Sayab, M., Karell, F., 2015. Near-orthogonal deformation successions in the poly-deformed Paleoproterozoic Martimo belt: implications for the tectonic evolution of Northern Fennoscandia. Precambrian Res. 270, 22–38.
Mukhopadhyay, D.K., Haimanot, B.W., 1989. Geometric analysis and significance of mesoscopic shear zones in the Precambrian gneisses around the Kolar Schist Belt, south India. J. Struct. Geol. 11, 569–581.
Neves, S.P., Mariano, G., 1999. Assessing the tectonic significance of a large-scale transcurrent shear zone system: the Pernambuco lineament, northeastern Brazil. J. Struct. Geol. 21, 1369–1383.
Neves, S.P., Silva, J.M.R., Mariano, G., 2005. Oblique lineations in orthogneisses and supracrustal rocks: vertical partitioning of strain in a hot crust (Borborema Province, NE Brazil). J. Struct. Geol. 27, 1513–1527.
Neves, S.P., Lages, G.A., Brasilino, R.G., Miranda, A.W.A., 2015. Paleoproterozoic accretionary and collisional processes and the build-up of the Borborema Province (NE Brazil): geochronological and geochemical evidence from the Central Domain. J. S. Am. Earth Sci. 58, 165–187.
Neves, S.P., Silva, J.M.R., Bruguier, O., 2017. Geometry, kinematics and geochronology of the Sertânia Complex (central Borborema Province, NE Brazil): assessing the role of accretionary versus intraplate processes during West Gondwana assembly. Precambrian Res. 298, 552–571.
Ramsay, J.G., 1967. Folding and Fracturing of Rocks. McGraw Hill, New York.
Ramsay, J.G., Huber, M.I., 1987. The Techniques of Modern Structural Geology, vol. 2 Folds and Fractures. Academic Press, London.
Santos, C.A., 2012. Cinturão de Cisalhamento Congo – Cruzeiro do Nordeste: Uma descontinuidade crustal no Domínio da Zona Transversal, Província Borborema. PhD thesis. Universidade Federal de Pernambuco 126 pp.
Santos, C.A., Accioly, A.C., 2010. Programa Geologia Do Brasil. Carta Geológica – Escala 1:100 000: Folha SC.24-x-b-i. CPRM – Serviço Geológico do Brasil, Sertânia.
Santos, E.J., Ferreira, C.A., Silva Jr., J.M.F., 2002. Geologia e Recursos Minerais do Estado da Paraíba. Programa Levantamentos Geológicos Básicos do Brasil. CPRM – Serviço Geológico do Brasil.
Santos, E.J., Nutman, A.P., Brito Neves, B.B., 2004. Idades SHRIMP U-Pb do Complexo Sertânia: implicações sobre a evolução tectônica da zona transversal, Província Borborema. Geol. Usp. Série Científica 4, 1–12.
Santos, L.C.M.L., Dantas, E.L., Santos, E.J., Santos, R.V., Lima, H.M., 2015. Early to late Paleoproterozoic magmatism in NE Brazil: the Alto Moxotó Terrane and its tectonic implications for the pre-West Gondwana assembly. J. S. Am. Earth Sci. 58, 188–209.
Santos, L.C.M.L., Dantas, E.L., Cawood, P.A., Santos, E.J., Fuck, R.A., 2017a. Neoarchean crustal growth and Paleoproterozoic reworking in the Borborema Province, NE Brazil: insights from geochemical and isotopic data of TTG and metagranitic rocks of the Alto Moxotó Terrane. J. S. Am. Earth Sci. 79, 342–363.
Santos, L.C.M.L., Dantas, E.L., Vidotti, R.M., Cawood, P.A., Santos, E.J., Fuck, R.A., Lima, H.M., 2017b. Two-stage terrane assembly in Western Gondwana: insights from structural geology and geophysical data of central Borborema Province, NE Brazil. J. Struct. Geol. 103, 167–184.

Silva, J.M.R., Mariano, G., 2000. Geometry and kinematics of the Afogados da Ingazeira shear zone, Northeast Brazil. Int. Geol. Rev. 42, 86–95.
Simón, J.L., 2004. Superposed buckle folding in the eastern Iberian Chain, Spain. J. Struct. Geol. 26, 1447–1464.
Thiessen, R., 1986. Two-dimensional refold interference patterns. J. Struct. Geol. 8, 563–573.
Van Kranendonk, M.J., Ivanic, T.J., Wingate, M.T.D., Kirkland, C.L., Wyche, S., 2013. Long-lived, autochthonous development of the Archean Murchison domain, and implications for Yilgarn Craton tectonics. Precambrian Res. 229, 49–92.
Vauchez, A., Neves, S.P., Caby, R., Corsini, M., Egydio-Silva, M., Arthaud, M.H., Amaro, V., 1995. The Borborema shear zone system, NE Brazil. J. S. Am. Earth Sci. 8, 247–266.
Zhang, J., Cunningham, D., 2012. Kilometer-scale refolded folds caused by strike-slip reversal and intraplate shortening in the Beishan region, China. Tectonics 31, TC3009. http://dx.doi.org/10.1029/2011TC003050.
Zheng, Y., Wang, T., Ma, M., Davis, G.A., 2004. Maximum effective moment criterion and the origin of low-angle normal faults. J. Struct. Geol. 26, 271–285.
Zheng, Y., Zhang, J., Wang, T., 2011. Puzzles and the maximum-effective-moment (MEM) criterion in structural geology. J. Struct. Geol. 33, 1394–1405.